DOI: 10.1021/ic100087d

Inorganic Chemistry
Article

Highly Convenient Regioselective Intermolecular Hydroamination of Alkynes Yielding Ketimines Catalyzed by Gold(I) Complexes of 1,2,4-triazole Based N-heterocyclic Carbenes

Chandrakanta Dash,[†] Mobin M. Shaikh,[‡] Ray J. Butcher,[§] and Prasenjit Ghosh*[,†]

[†]*Department of Chemistry, and* [‡]*National Single Crystal X-ray Diffraction Facility, Indian Institute of Technology Bombay, Powai, Mumbai 400 076, India, and* [§]*Department of Chemistry, Howard University, Washington, D.C. 20059*

Received January 15, 2010

A series of highly efficient gold(I) precatalysts of 1,2,4-triazole based N-heterocyclic carbenes, [1-R-4-R′-1,2,4-triazol-5-ylidene]AuCl [R = CH_2CO^tBu, R′ = CH_2Ph (**1c**); R = CH_2CONH^tBu, R′ = CH_2Ph (**2c**); R = CH_2CO^tBu, R′ = CH_2CO^tBu (**3c**), and R = $C_6H_{10}OH$, R′ = CH_2Ph (**4c**)] are reported for the hydroamination of terminal alkynes with a variety of sterically demanding *o*/*p*-substituted aryl amines yielding the corresponding ketimines in air. The gold **1c**−**4c** complexes exhibited extremely high activity in comparison to the silver analogues **1b**−**4b**, thereby highlighting the role of gold as a metal in the catalysis of the hydroamination reaction. Additionally, the 1,2,4-triazole based **1c**−**4c** precatalysts showed significantly superior activity in comparison to the two representative imidazole analogues, namely, [1-(benzyl)-3-(*N*-*t*-butylacetamido)imidazol-2-ylidene]AuCl and [1-(2-hydroxy-cyclohexyl)-3-(benzyl)imidazol-2-ylidene]AuCl, thereby underscoring the importance of the 1,2,4-triazole based N-heterocyclic carbenes over the imidazole based ones in designing the gold(I) precatalysts for the hydroamination reaction. The gold(I) complexes (**1c**−**4c**) were synthesized by transmetalation reaction of the silver analogues **1b**−**4b** with $(SMe_2)AuCl$ in 60−76% yield while the silver **1b**−**4b** complexes in turn were synthesized from the respective 1,2,4-triazolium halide salts by treatment with Ag_2O in 43−64% yield.

Introduction

The hydroamination of unsaturated substrates like the alkynes and alkenes provide a fundamentally simple, atom economic approach for the efficient construction of the C−N bonds, which together with C−C bond formation lie at the heart of organic synthesis and undoubtedly are among the core challenges of the contemporary organic synthesis today.[1] Thus, finding novel and convenient ways of forming these bonds are in obvious demand. In this regard the catalytic hydroamination of alkynes yields reactive but synthetically useful ketimines and enamines that are often the key intermediates to numerous nitrogen containing compounds of medicinal, agrochemical, and industrial interest.[2] It is distinctly superior to the other available methods like imination of ketones[3] or the aminomercuration/demercuration of alkynes[4] that involve the stoichiometric use of toxic mercury reagents. The hydroamination of alkynes have been successfully employed as key steps in a variety of total syntheses of target molecules.[5] The amines and the alkynes being both inexpensive and readily available, at least in the laboratory scale, have largely contributed to the rising popularity of the reaction in recent times. Furthermore, the alkyne hydroamination is more facile compared to the alkene hydroamination for reasons of the alkynes being sterically less demanding and also for its π-bond being about 70 kJ/mol weaker than that in alkenes.[6]

The hydroamination reaction, with all its advantages though provide an enticing option, possesses an inherent barrier for the reaction to occur owing to electrostatic reasons as both of the substrates, namely, the amine and the alkyne or

*To whom correspondence should be addressed. E-mail: pghosh@chem.iitb.ac.in. Fax: +91-22-2572-3480.

(1) (a) Severin, R.; Doye, S. *Chem. Soc. Rev.* **2007**, *36*, 1407–1420. (b) Pohlki, F.; Doye, S. *Chem. Soc. Rev.* **2003**, *32*, 104–114. (c) Müller, T. E.; Beller, M. *Chem. Rev.* **1998**, *98*, 675–703.

(2) (a) Hodgson, D. M.; Kaka, N. S. *Angew. Chem.* **2008**, *120*, 10106–10108. (b) Mukherjee, S.; Yang, J. W.; Hoffmann, S.; List, B. *Chem. Rev.* **2007**, *107*, 5471–5569. (c) Spino, C. *Angew. Chem., Int. Ed.* **2004**, *43*, 1764–1766.

(3) Layer, R. W. *Chem. Rev.* **1963**, *63*, 489–510.

(4) (a) Larock, R. C. *Angew. Chem., Int. Ed. Engl.* **1978**, *17*, 27–37. (b) Barluenga, J.; Aznar, F. *Synthesis* **1975**, 704–705.

(5) (a) Trost, B. M.; Fandrick, D. R. *Org. Lett.* **2005**, *7*, 823–826. (b) Mujahidin, D.; Doye, S. *Eur. J. Org. Chem.* **2005**, 2689–2693. (c) Patil, N. T.; Pahadi, N. K.; Yamamoto, Y. *Tetrahedron Lett.* **2005**, *46*, 2101–2103.

(6) Straub, T.; Haskel, A.; Neyroud, T. G.; Kapon, M.; Botoshansky, M.; Eisen, M. S. *Organometallics* **2001**, *20*, 5017–5035.

Published on Web 04/29/2010

the alkene, are considered electron rich and, thus, calls for the participation of metals in catalyzing the reaction by employing various activation pathways.[1a,7] The metals on their part facilitate the catalysis by activating either the amine or the C−C multiple bonded substrate and upon subsequent protonolysis yields the desired product alongside regenerating back the catalyst. Depending upon the choice of the metal though, the catalytic hydroamination reaction can often be air and moisture sensitive and thus be difficult to handle as is mostly the case with the lanthanides, the alkali metals and the early transition metals that are generally known to function by the amine activation pathway.[7a,8] In this regard, notable are the late transition metals, which being less oxophilic are less sensitive to air and moisture, exhibit desirable traits for utility in the hydroamination catalysis, and have been reported to function by the alkyne activation pathway.[9] Gold being one such metal, long known as an inert coinage metal with little catalytic properties and whose catalytic exploits are of recent interest,[10] we became interested in exploring its utility in the hydroamination reaction. We rationalized that gold, in both of its (I) and (III) oxidation states, is known for its high carbophilicity and diminished oxophilicity and is thus well suited for catalyzing the hydroamination reaction most likely by an alkyne activation pathway involving the nucleophilic attack by an amine.[11]

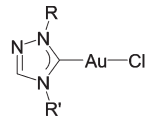

R = CH_2CO^tBu, R' = CH_2Ph (**1c**)
R = CH_2CONH^tBu, R' = CH_2Ph (**2c**)
R = CH_2CO^tBu, R' = CH_2CO^tBu (**3c**)
R = $C_6H_{10}OH$, R' = CH_2Ph (**4c**)

Figure 1

Our long-standing interest remains in exploring the utility of N-heterocyclic carbenes[12] in biomedical applications[13] as well as in chemical catalysis particularly that range from producing biodegradable polymers by the ring-opening polymerization of L-lactide,[10f,h,14] to a variety of C−C bond forming reactions like the Pd mediated Suzuki,[15] Sonogashira,[16] and the Hiyama[16c] couplings and in Ni mediated base-free Michael addition reactions.[17] Furthermore, having successfully employed imidazole derived N-heterocyclic carbene precatalysts in C−C bond forming reactions, we decided to extend our study to C−N bond forming reactions and particularly do so by employing the much less explored 1,2,4-triazole derived N-heterocyclic carbenes[18] that provide new steric and electronic environments compared to the imidazole counterparts. Our specific aim was in gauging the potential of the 1,2,4-triazole derived N-heterocyclic carbenes in catalysis by performing a comparative study with respect to the extensively studied imidazole derived N-heterocyclic carbenes. Specifically, we decided to explore the potentials of gold complexes of 1,2,4-triazole based N-heterocyclic carbenes in the alkyne hydroamination reactions.

Here in this contribution, we report a series of highly efficient gold(I) precatalysts, **1c**−**4c**, of 1,2,4-triazole based N-heterocyclic carbenes for the hydroamination of terminal alkynes with aryl amines yielding the ketimines in air (Figure 1, eq 1).

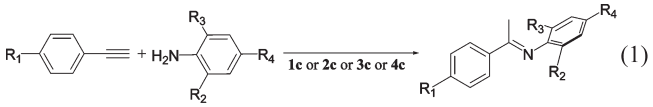

(1)

R_1 = H, Me
R_2 = H, Me, Et, ^{i}Pr
R_3 = Me, Et, ^{i}Pr
R_4 = H, Me

Furthermore, we performed a comparison of the catalytic activity of the gold(I) precatalysts, **1c**−**4c**, with their silver analogues **1b**−**4b** as well as with the gold(I) imidazole-based N-heterocyclic carbene counterparts of **2c** and **4c**, namely, the [1-(benzyl)-3-(*N*-*t*-butylacetamido)imidazol-2-ylidene]AuCl[12c]

(7) (a) Ryu, J.-S.; Li, G. Y.; Marks, T. J. *J. Am. Chem. Soc.* **2003**, *125*, 12584–12605. (b) Müller, T. E.; Grosche, M.; Herdtweck, E.; Pleier, A.-K.; Walter, E.; Yan, Y.-K. *Organometallics* **2000**, *19*, 170–183.

(8) (a) Kim, H.; Livinghouse, T.; Seomoon, D.; Lee, P. H. *Bull. Korean Chem. Soc.* **2007**, *28*, 1127–1134. (b) Ackermann, L.; Bergman, R. G.; Loy, R. N. *J. Am. Chem. Soc.* **2003**, *125*, 11956–11963. (c) Haak, E.; Bytschkov, I.; Doye, S. *Angew. Chem., Int. Ed.* **1999**, *38*, 3389–3391.

(9) (a) Shanbhag, G. V.; Halligudi, S. B. *J. Mol. Catal. A: Chem.* **2004**, *222*, 223–228. (b) Müller, T. E.; Pleier, A.-K. *J. Chem. Soc., Dalton Trans.* **1999**, 583–587.

(10) (a) Lin, J. C. Y.; Huang, R. T. W.; Lee, C. S.; Bhattacharyya, A.; Hwang, W. S.; Lin, I. J. B. *Chem. Rev.* **2009**, *109*, 3561–3598. (b) Marion, N.; Ramón, R. S.; Nolan, S. P. *J. Am. Chem. Soc.* **2009**, *131*, 448–449. (c) Brown, T. J.; Dickens, M. G.; Widenhoefer, R. A. *J. Am. Chem. Soc.* **2009**, *131*, 6350–6351. (d) Ramón, R. S.; Marion, N.; Nolan, S. P. *Chem.—Eur. J.* **2009**, *15*, 8695–8697. (e) Marion, N.; Nolan, S. P. *Chem. Soc. Rev.* **2008**, *37*, 1776–1782. (f) Ray, L.; Katiyar, V.; Barman, S.; Raihan, M. J.; Nanavati, H.; Shaikh, M. M.; Ghosh, P. *J. Organomet. Chem.* **2007**, *692*, 4259–4269. (g) Marion, N.; Gealageas, R.; Nolan, S. P. *Org. Lett.* **2007**, *9*, 2653–2656. (h) Ray, L.; Katiyar, V.; Raihan, M. J.; Nanavati, H.; Shaikh, M. M.; Ghosh, P. *Eur. J. Inorg. Chem.* **2006**, 3724–3730. (i) de Frémont, P.; Stevens, E. D.; Fructos, M. R.; Díaz-Requejo, M. M.; Pérez, P. J.; Nolan, S. P. *Chem. Commun.* **2006**, 2045–2047. (j) Bender, C. F.; Widenhoefer, R. A. *Org. Lett.* **2006**, *8*, 5303–5305. (k) Marion, N.; Díez-González, S.; de Frémont, P.; Noble, A. R.; Nolan, S. P. *Angew. Chem., Int. Ed.* **2006**, *45*, 3647–3650. (l) Fructos, M. R.; de Frémont, P.; Nolan, S. P.; Díaz-Requejo, M. M.; Pérez, P. J. *Organometallics* **2006**, *25*, 2237–2241. (m) Marion, N.; de Frémont, P.; Lemiére, G.; Stevens, E. D.; Fensterbank, L.; Malacria, M.; Nolan, S. P. *Chem. Commun.* **2006**, 2048–2050. (n) Fructos, M. R.; Belderrain, T. R.; de Frémont, P.; Scott, N. M.; Nolan, S. P.; Díaz-Requejo, M. M.; Pérez, P. J. *Angew. Chem., Int. Ed.* **2005**, *44*, 5284–5288. (o) Lin, I. J. B.; Vasam, C. S. *Can. J. Chem.* **2005**, *83*, 812–825.

(11) (a) Lavallo, V.; Frey, G. D.; Donnadieu, B.; Soleilhavoup, M.; Bertrand, G. *Angew. Chem., Int. Ed.* **2008**, *47*, 5224–5228. (b) Zhang, Y.; Donahue, J. P.; Li, C.-J. *Org. Lett.* **2007**, *9*, 627–630. (c) Widenhoefer, R. A.; Han, X. *Eur. J. Org. Chem.* **2006**, 4555–4563.

(12) (a) Samantaray, M. K.; Pang, K.; Shaikh, M. M.; Ghosh, P. *Dalton Trans.* **2008**, 4893–4902. (b) Samantaray, M. K.; Pang, K.; Shaikh, M. M.; Ghosh, P. *Inorg. Chem.* **2008**, *47*, 4153–4165. (c) Ray, L.; Shaikh, M. M.; Ghosh, P. *Inorg. Chem.* **2008**, *47*, 230–240. (d) Samantaray, M. K.; Roy, D.; Patra, A.; Stephen, R.; Saikh, M.; Sunoj, R. B.; Ghosh, P. *J. Organomet. Chem.* **2006**, *691*, 3797–3805.

(13) (a) Ray, S.; Asthana, J.; Tanski, J. M.; Shaikh, M. M.; Panda, D.; Ghosh, P. *J. Organomet. Chem.* **2009**, *694*, 2328–2335. (b) Ray, S.; Mohan, R.; Singh, J. K.; Samantaray, M. K.; Shaikh, M. M.; Panda, D.; Ghosh, P. *J. Am. Chem. Soc.* **2007**, *129*, 15042–15053.

(14) (a) Samantaray, M. K.; Katiyar, V.; Pang, K.; Nanavati, H.; Ghosh, P. *J. Organomet. Chem.* **2007**, *692*, 1672–1682. (b) Samantaray, M. K.; Katiyar, V.; Roy, D.; Pang, K.; Nanavati, H.; Stephen, R.; Sunoj, R. B.; Ghosh, P. *Eur. J. Inorg. Chem.* **2006**, 2975–2984.

(15) (a) Kumar, S.; Shaikh, M. M.; Ghosh, P. *J. Organomet. Chem.* **2009**, *694*, 4162–4169. (b) Ray, L.; Shaikh, M. M.; Ghosh, P. *Organometallics* **2007**, *26*, 958–964. (c) Ray, L.; Shaikh, M. M.; Ghosh, P. *Dalton Trans.* **2007**, 4546–4555.

(16) (a) John, A.; Shaikh, M. M.; Ghosh, P. *Dalton Trans.* **2009**, 10581–10591. (b) Samantaray, M. K.; Shaikh, M. M.; Ghosh, P. *J. Organomet. Chem.* **2009**, *694*, 3477–3486. (c) Dash, C.; Shaikh, M. M.; Ghosh, P. *Eur. J. Inorg. Chem.* **2009**, 1608–1618. (d) Ray, L.; Barman, S.; Shaikh, M. M.; Ghosh, P. *Chem.—Eur. J.* **2008**, *14*, 6646–6655.

(17) (a) Samantaray, M. K.; Shaikh, M. M.; Ghosh, P. *Organometallics* **2009**, *28*, 2267–2275. (b) Ray, S.; Shaikh, M. M.; Ghosh, P. *Eur. J. Inorg. Chem.* **2009**, 1932–1941.

(18) Dash, C.; Shaikh, M. M.; Butcher, R. J.; Ghosh, P. *Dalton Trans.* **2010**, *39*, 2515–2524.

Scheme 1

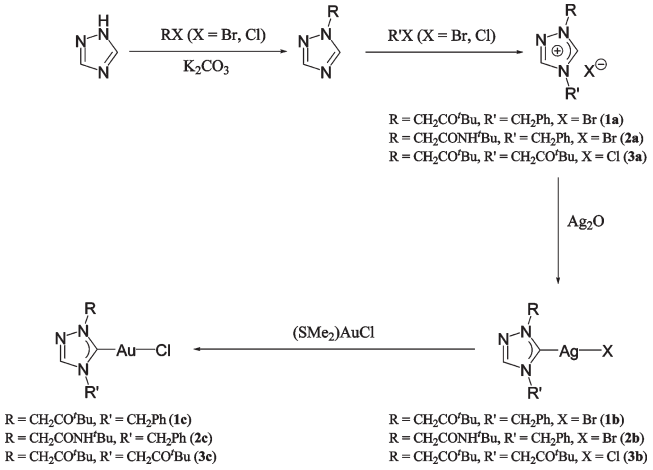

and [1-(2-hydroxy-cyclohexyl)-3-(benzyl)imidazol-2-ylidene]AuCl[10f] complexes to highlight the superiority of the gold(I) precatalysts (**1c**−**4c**) of 1,2,4-triazole derived N-heterocyclic carbenes in the alkyne hydroamination reaction. Additionally, the density functional theory (DFT) studies performed on the **1c**−**4c** complexes revealed the 1,2,4-triazole based N-heterocyclic carbenes to be strongly σ-donating ligands with very little π-back bonding tendencies similar to the much studied imidazole based N-heterocyclic carbene counterparts.

Results and Discussion

A series of gold(I) precatalysts, **1c**−**4c**, supported over new *N*/*O*-functionalized 1,2,4-triazolium N-heterocyclic carbene ligands, namely, [1-R-4-R′-1,2,4-triazol-5-ylidene]AuCl [R = CH_2CO^tBu, R′ = CH_2Ph (**1c**); R = CH_2CONH^tBu, R′ = CH_2Ph (**2c**); R = CH_2CO^tBu, R′ = CH_2CO^tBu (**3c**), and R = $C_6H_{10}OH$, R′ = CH_2Ph (**4c**)] were designed for studying the intermolecular hydroamination of alkynes. In particular, the *N*/*O*-functionalized 1,2,4-triazolium halide salts (**1a**−**4a**) were synthesized by the alkylation reaction of the appropriately substituted 1,2,4-triazoles in 44−70% yield (Schemes 1 and 2). The formation of **1a**−**4a** was very much evident from the respective ^{1}H NMR spectrum in which the characteristic 1,2,4-triazolium NC(5)*H*N resonance appeared at 10.6−11.1 ppm, at a significantly downfield shifted region compared to the imidazole based counterparts, NC(2)*H*N, at about 9.70−10.1 ppm.[10f,12b,c]

The treatment of **1a**−**4a** with Ag_2O resulted in the silver complexes **1b**−**4b** in 43−64% yield (Schemes 1 and 2) by following the convenient methodology developed by Lin and co-workers[19] and, as expected, the $^{13}C\{^1H\}$ NMR spectrum showed a new peak at about 184.4−187.9 ppm attributable to the metal bound 1,2,4-triazolium carbene moiety ($C_{carbene}$−Ag). In this regard it is noteworthy that similar chemical shifts have been reported for other 1,2,4-triazole based N-heterocyclic carbene complexes, namely, [{(1,2-*di*-methyl-4-(*i*-propyl)-1,2,4-triazol-3,5-diylidene)-Ag}$^+$TfO$^-$]$_n$ [182.9 ppm][20] and [{*bis*(4-benzyl-1,2,4-triazol-5-ylidene)}dihydroborate]$_2$Ag$_2$ [189.3 ppm].[21]

(19) Wang, H. M. J.; Lin, I. J. B. *Organometallics* **1998**, *17*, 972–975.
(20) Guerret, O.; Solé, S.; Gornitzka, H.; Teichert, M.; Trinquier, G.; Bertrand, G. *J. Am. Chem. Soc.* **1997**, *119*, 6668–6669.

Scheme 2

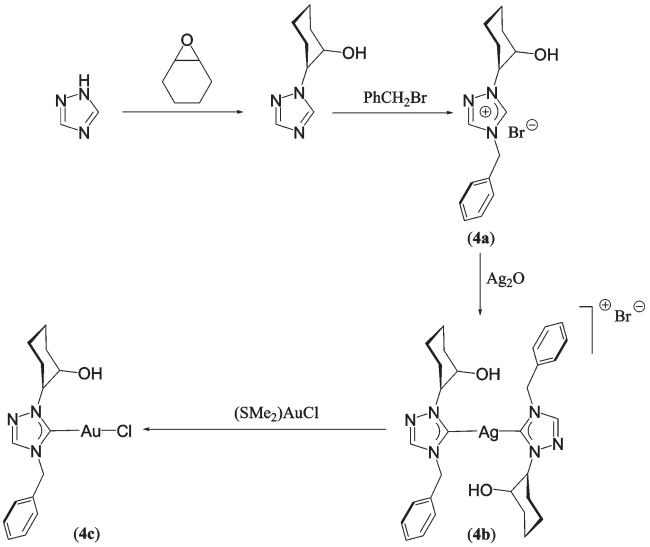

Finally, the gold(I) **1c**−**4c** precatalysts were synthesized by the transmetalation reaction of silver complexes (**1b**−**4b**) with $(SMe_2)AuCl$ in 60−76% yield and was accompanied by the precipitation of an off-white silver halide salt. The observed 1,2,4-triazolium $C_{carbene}$−Au peak at 175.8−177.2 ppm in the **1c**−**4c** complexes compared well with the other reported gold(I) 1,2,4-triazole based N-heterocyclic carbene complexes, namely, [1,4-*bis*(methyl)-1,2,4-triazol-5-ylidene]AuCl [173.0 ppm][22] and [2-phenyl-6,7-dihydro-5*H*-pyrrolo-[2,1-*c*]-[1,2,3]triazol-2-ylidene]AuCl [167.8 ppm].[23] Quite interestingly, the 1,2,4-triazole $C_{carbene}$−Au (N*C*N) resonances at 175.8−177.2 ppm for the **1c**−**4c** complexes were significantly upfield shifted compared to its immediate silver(I) counterparts **1b**−**4b** at 184.4−187.9 ppm. A similar trend is also observed for the imidazole based N-heterocyclic carbene complexes of gold and silver, for example, the $C_{carbene}$−Au (N*C*N) resonance for [1-(2-hydroxy-cyclohexyl)-3-(benzyl)imidazol-2-ylidene]AuCl appeared at 170.1 ppm while the $C_{carbene}$−Ag (N*C*N) peak for {[1-(2-hydroxy-cyclohexyl)-3-(benzyl)imidazol-2-ylidene]$_2$-Ag}$^+$Cl$^-$ appeared at 179.7 ppm.[10f]

The molecular structure determination by X-ray crystallography revealed these gold(I) precatalysts, **1c**−**4c**, to be discrete monomers in keeping with their intended use as single-site catalysts for the study of intermolecular hydroamination of terminal alkynes. For comparison, when the molecular structures of two representative silver(I) analogues, **1b** and **2b**, were determined, the **1b** complex was found to be dimeric while the other **2b** complex was monomeric quite similar to the gold(I) analogues, **1c**−**4c**, (Figures 2−5 and Supporting Information, Figures S1−S2). All of the monomeric gold(I) (**1c**−**4c**) and silver(I) (**2b**) complexes displayed a linear geometry [$\angle$ $C_{carbene}$−M−X; M = Au, X = Cl, 176.0(2)−178.3(3)°, M = Ag, X = Br, 170.35(8)°] at the metal consistent with a two coordinated d^{10} metal center, while the **1b** complex showed a slightly deviated geometry [$\angle C_{carbene}$−Ag−Br = 157.93(13)°] as a result of coordination

(21) Papini, G.; Bandoli, G.; Dolmella, A.; Lobbia, G. G.; Pellei, M.; Santini, C. *Inorg. Chem. Commun.* **2008**, *11*, 1103–1106.
(22) Wang, H. M. J.; Vasam, C. S.; Tsai, T. Y. R.; Chen, S.-H.; Chang, A. H. H.; Lin, I. J. B. *Organometallics* **2005**, *24*, 486–493.
(23) de Frémont, P.; Scott, N. M.; Stevens, E. D.; Nolan, S. P. *Organometallics* **2005**, *24*, 2411–2418.

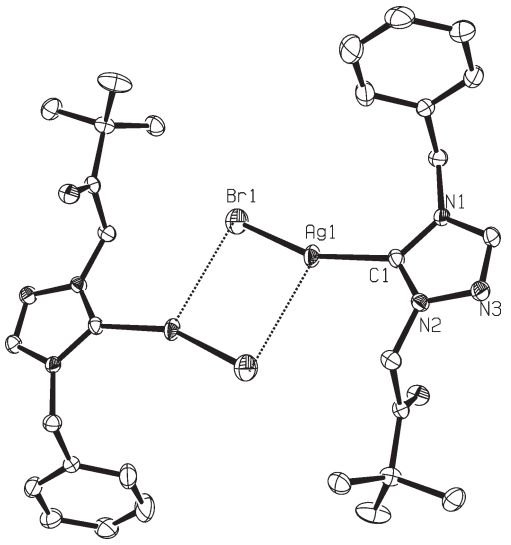

Figure 2. ORTEP drawing of **1b** with thermal ellipsoids shown at the 50% probability level. Selected bond lengths (Å) and angles (deg): Ag1−C1 2.092(4), Ag1−Br1 2.4629(9), N1−C1 1.349(5), N2−C1 1.327(6), C1−Ag1−Br1 157.93(13), N1−C1−N2 103.0(4).

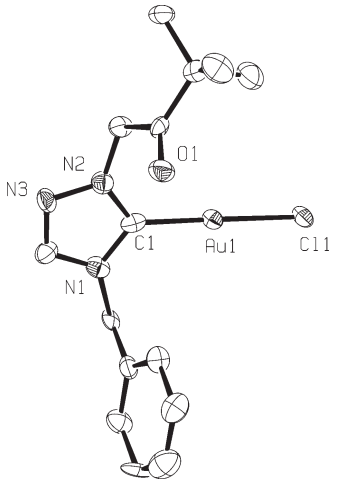

Figure 3. ORTEP drawing of **1c** with thermal ellipsoids shown at the 50% probability level. Selected bond lengths (Å) and angles (deg): Au1−C1 1.972(12), Au1−Cl1 2.269(3), N1−C1 1.355(15), N2−C1 1.325(14), C1−Au1−Cl1 177.7(4), N1−C1−N2 104.0(10).

from an additional bridging bromine atom. The $C_{carbene}$−M bond distances [M = Au; 1.950(10)−1.984(9) Å and Ag; 2.092(4)−2.092(7) Å] are slightly shorter than the sum of individual covalent radii of the bonding atoms [C−Au = 2.108 Å and C−Ag = 2.111 Å][24] but compare well with the other reported gold(I) and silver(I) 1,2,4-triazole N-heterocyclic carbene complexes, namely, [1,4-*bis*(methyl)-1,2,4-triazol-5-ylidene]AuCl [1.71(8) Å],[22] [2-phenyl-6,7-dihydro-5*H*-pyrrolo-[2,1-*c*][1,2,3]triazol-2-ylidene]AuCl [1.979(5) Å],[23] and [{(1,2-*di*-methyl-4-(*i*-propyl)-1,2,4-triazol-3,5-diylidene)-Ag}$^{+}$TfO^{-}]$_n$ [2.086(4) Å],[20] and so forth. Consistent with the smaller covalent radii of Au [1.37 Å] compared to Ag [1.46 Å],[25] the $C_{carbene}$−Au distances [1.950(10)−1.984(9) Å]

(24) Pauling, L. *The Nature of Chemical Bond*, 3rd ed.; Cornell University Press: Ithaca, NY, 1960; pp 256−257.

(25) Tripathi, U. M.; Bauer, A.; Schmidbaur, H. *Dalton Trans.* **1997**, 2865–2868.

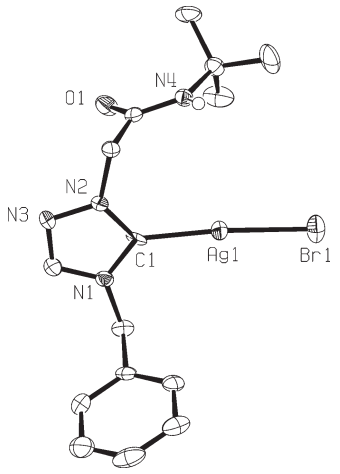

Figure 4. ORTEP drawing of **2b** with thermal ellipsoids shown at the 50% probability level. Selected bond lengths (Å) and angles (deg): Ag1−C1 2.092(7), Ag1−Br1 2.4614(9), N1−C1 1.360(8), N2−C1 1.337(9), C1−Ag1−Br1 170.35(8), N1−C1−N2 101.5(6).

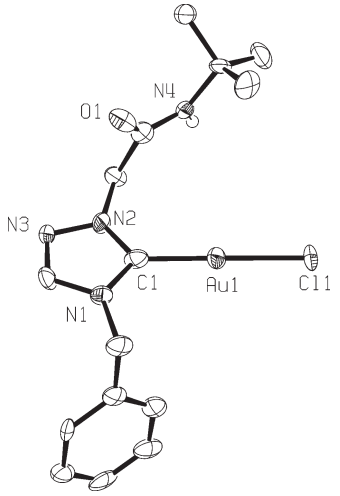

Figure 5. ORTEP drawing of **2c** with thermal ellipsoids shown at the 50% probability level. Selected bond lengths (Å) and angles (deg): Au1−C1 1.950(10), Au1−Cl1 2.319(3), N1−C1 1.391(12), N2−C1 1.358(12), C1−Au1−Cl1 178.3(3), N1−C1−N2 101.1(8).

in **1c**−**4c** are indeed shorter than the $C_{carbene}$−Ag distances [2.092(4)−2.092(7) Å] in the **1b** and **2b** complexes.

The nature of M−NHC (M = Ag, Au) interaction in the gold(I) **1c**−**4c** and silver(I) **1b** and **2b** complexes were investigated using a DFT study. Specifically, the geometry optimized structures of the **1b**, **2b**, and **1c**−**4c** were obtained from X-ray coordinates followed by single point calculations at B3LYP/SDD, 6-31G(d) level of theory (Supporting Information, Tables S2−S6). The Natural Bond Orbital (NBO) calculations were performed on these computed structures to gain understanding on the electronic structure of these complexes. Quite interestingly, both the Mulliken and natural charge analyses showed that binding of the free 1,2,4-triazole based N-heterocyclic carbene fragment to the metal center in these complexes, led to significant increase in its electron density with concomitant decrease in the electron density on the carbene carbon with respect to the free 1,2,4-triazole NHC fragment (Supporting Information Tables S7−S12). Further Natural Bond Orbital (NBO) analysis revealed that the electron donation occurred on to the *5s*

orbital of silver in the **1b** and **2b** complexes while to the *6s* orbital of gold in the **1c**−**4c** complexes (Supporting Information, Tables S13−S14). A careful scrutiny of the NBO results indicated that the Au−$C_{carbene}$ bond in **1c**−**4c** is composed of an interaction of a C_{sp_2} orbital of the 1,2,4-triazole based NHC ligand with an sd orbital of the metal center (Supporting Information, Table S15).

A glimpse of the σ−donating character of the 1,2,4-triazole based NHC ligand could be obtained by the Charge Decomposition Analysis (CDA) studies carried out on the silver **1b**−**2b** and the gold **1c**−**4c** complexes using the AOMix-CDA software, that estimated the extent of the σ−donation (*d*)

$$\mathrm{NHC} \xrightarrow{\sigma} \mathrm{MX(M = Ag, Au)}$$

and π−back-donation (*b*)

$$\mathrm{NHC} \xleftarrow{\pi} \mathrm{MX(M = Ag, Au)}$$

occurring in these complexes. The high *d*/*b* ratio of 5.14−4.95 in gold **1c**−**4c** and of 7.66−6.96 in silver **1b** and **2b** complexes indicate strong σ−donating nature of the 1,2,4-triazole based N-heterocyclic carbene ligands in parallel to that seen for imidazole based N-heterocyclic carbenes (Supporting Information, Table S16) in the gold(I) complexes, namely, [1-(benzyl)-3-(*N*-*t*-butylacetamido)imidazol-2-ylidene]AuCl [4.49],[12c] [1-(*i*-propyl)-3-{*N*-(*t*-butylacetamido)imidazol-2-ylidene}]$_2$-Au^+Cl^- [5.23],[12b] and in the silver(I) complexes, namely, [1-(benzyl)-3-(*N*-*t*-butylacetamido)imidazol-2-ylidene]AgCl [8.18],[12c] [1-(*i*-propyl)-3-{*N*-(t-butylacetamido)imidazol-2-ylidene}]$_2Ag^+Cl^-$ [11.44].[12b]

Further insight into the nature of NHC−M (M = Ag and Au) σ−interaction could be obtained by constructing the molecular orbital (MO) correlation diagram from the individual fragment molecular orbitals (FMOs) of the 1,2,4-triazole based NHC ligand and the MX (M = Ag and Au) fragments. Quite interestingly, the molecular orbital (MO) depicting the σ−interaction in the gold(I) **1c** [HOMO−8, HOMO−9, and HOMO−28], **2c** [HOMO−8, HOMO−10, and HOMO−32], **3c** [HOMO−6, HOMO−7, and HOMO−28], and **4c** [HOMO−7, HOMO−8, and HOMO−29] complexes and in the silver(I) **1b** [HOMO−6 and HOMO−24] and **2b** [HOMO−7 and HOMO−25] complexes were found to be deeply buried thereby indicating the significantly stable nature of the NHC−M (M = Ag, Au) interaction analogous to the imidazole based NHC−M σ−interacting molecular orbital (MO) of gold(I) and silver(I) complexes[12b,c] (Figure 6 and Supporting Information, Figures S3−S13). In this regard it is worth noting that the well-known Schrock and Fischer carbenes are very much susceptible to the electrophilic and nucleophilic attacks unlike the N-heterocyclic carbene complexes.[26]

Lastly, the strength of the NHC−M (M = Ag, Au) interaction, estimated by computing NHC−M (M = Ag, Au) bond dissociation energy (D_e) at B3LYP/SDD, 6-31G(d) level of the theory for the gold **1c** [79.7 kcal/mol], **2c** [81.0 kcal/mol], **3c** [80.7 kcal/mol], and **4c** [81.2 kcal/mol] and the silver **1b** [56.7 kcal/mol] and **2b** [58.5 kcal/mol] complexes (Supporting Information, Table S17) were found to be weaker than that estimated for gold(I) and silver(I) complexes of imidazole based N-heterocyclic carbenes, namely, [1-(benzyl)-3-(*N*-*t*-butylacetamido)imidazol-2-ylidene]AuCl [D_e: 82.7 kcal/mol][12c] and [1-(benzyl)-3-(*N*-*t*-butylacetamido)imidazol-2-ylidene]AgCl [D_e: 62.2 kcal/mol].[12c]

Significantly enough, the gold(I) **1c**−**4c** complexes displayed good to high activity for the intermolecular hydroamination reaction of *o*/*p*-substituted aryl amines with terminal alkynes in air. Specifically, when terminal alkynes like, phenylacetylene, 4-ethynyl toluene were treated with *o*/*p*-substituted aryl amines, namely, 2-methylaniline, 2,6-dimethylaniline, mesitylaniline, 2,6-diethylaniline, and 2,6-di-*i*-propylaniline at 2 mol % of the precatalyst loading in presence of 1 equiv of $AgBF_4$ in air, good to excellent conversion (42−93%) were obtained in 12 h at 90 °C. In this context it is worth noting that there have been prior reports of the use of gold(I) N-heterocyclic carbene complexes for the hydroamination reactions at the temperature range 40−200 °C.[11a,27] Quite interestingly, the similar catalysis runs performed with the silver(I) **1b**−**4b** complexes gave extremely subdued conversions (0−29%), thereby highlighting the role of gold in catalysis. Further comparison with the control experiments performed with $(SMe_2)AuCl$ in the presence of $AgBF_4$ and also with the corresponding blank experiment carried out with only $AgBF_4$ showed significant amplification of up to 85% under analogous conditions in case of the gold **1c**−**4c** precatalysts (Supporting Information, Table S18), thus underscoring the significance of 1,2,4-triazole based gold **1c**−**4c** precatalysts in the hydroamination reaction. Moreover, another control experiment performed with a representative 1,2,4-triazole based N-heterocyclic carbene generated in situ by treating the 1,2,4-triazolium bromide salt (**1a**) with KO^tBu or Et_3N showed no conversions for two representative substrates (Supporting Information, Table S19) thereby ruling out the possibility of the presence of the decomposed ligand behind the observed catalysis.

To investigate the regiochemistry of the hydroamination reaction, the isolation and subsequent characterization of the final products were carried out for a representative precatalyst **1c**. The hydroaminated products of the addition reaction showed Markovnikov type N−H addition across the alkyne substrates. Lastly, to verify the homogeneous nature of catalysis, the mercury drop test[28] showed no significant decrease in the product yields under the same conditions.

Important is the comparison of these gold(I) 1,2,4-triazole based (**1c**−**4c**) precatalysts with their imidazole-based counterparts. Indeed, the 1,2,4-triazole based gold(I) (**1c**−**4c**) complexes showed significantly higher activity compared to the two representative imidazole derived analogues, namely, [1-(benzyl)-3-(*N*-*t*-butylacetamido)imidazol-2-ylidene]AuCl[12c] and [1-(2-hydroxy-cyclohexyl)-3-(benzyl)imidazol-2-ylidene]AuCl,[10f] thereby highlighting the influence of 1,2,4-triazol-5-ylidene

(26) (a) Valyaev, D. A.; Peterleitner, M. G.; Leont'eva, L. I.; Novikova, L. N.; Semeikin, O. V.; Khrustalev, V. N.; Antipin, M. Y.; Ustynyuk, N. A.; Skelton, B. W.; White, A. H. *Organometallics* **2003**, *22*, 5491–5497. (b) Esteruelas, M. A.; González, A. I.; López, A. M.; Oñate, E. *Organometallics* **2003**, *22*, 414–425. (c) Raubenheimer, H. G.; Esterhuysen, M. W.; Timoshkin, A.; Chen, Y.; Frenking, G. *Organometallics* **2002**, *21*, 3173–3181. (d) Barluenga, J.; Flórez, J.; Fañanás, F. J. *J. Organomet. Chem.* **2001**, *624*, 5–17. (e) Barluenga, J.; Trabanco, A. A.; Flórez, J.; García-Granda, S.; Martín, E. *J. Am. Chem. Soc.* **1996**, *118*, 13099–13100. (f) Padolik, L. L.; Gallucci, J. C.; Wojcicki, A. *J. Am. Chem. Soc.* **1993**, *115*, 9986–9996.

(27) Zeng, X.; Frey, G. D.; Kousar, S.; Bertrand, G. *Chem.—Eur. J.* **2009**, *15*, 3056–3060.

(28) (a) Widegren, J. A.; Bennett, M. A.; Finke, R. G. *J. Am. Chem. Soc.* **2003**, *125*, 10301–10310. (b) Widegren, J. A.; Finke, R. G. *J. Mol. Catal. A: Chem.* **2003**, *198*, 317–341.

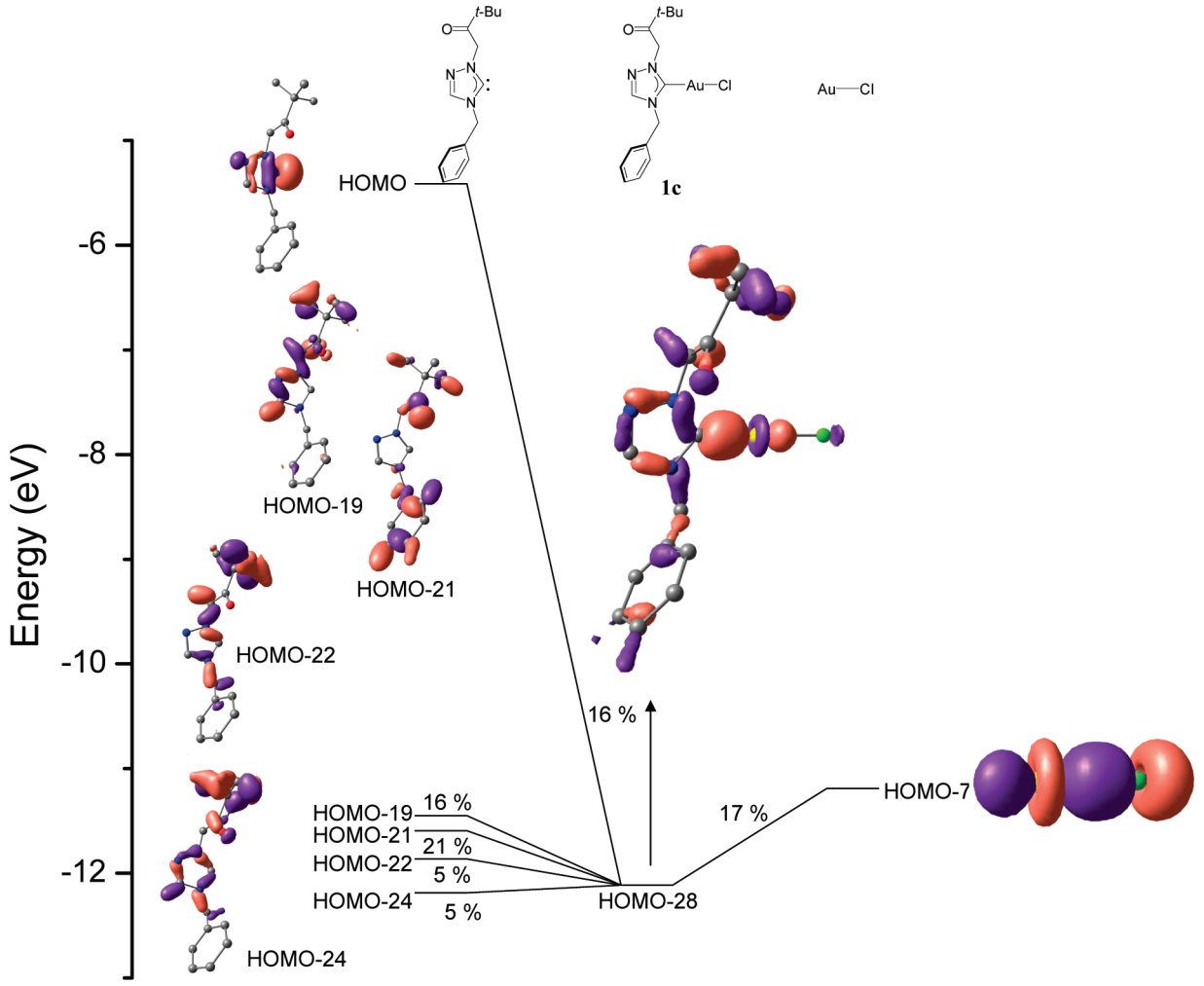

Figure 6. Simplified orbital interaction diagram showing the major contributions of the NHC-gold bond in **1c**.

ligands in stabilizing these highly efficient gold(I) **1c**−**4c** precatalysts. A 2−4 fold improvement in the product yield were observed for the 1,2,4-triazole based **1c**−**4c** precatalysts. Significantly enough, apart from our present study of the use of 1,2,4-triazole derived N-heterocyclic carbene precatalysts, **1c**−**4c**, for the intermolecular hydroamination of terminal alkynes, we are aware of only two reports of the use of N-heterocyclic carbene ligands in the terminal alkyne hydroamination reaction. For example, a cationic gold(I) complex of cyclic (alkyl)(amino)carbene (CAAC) displayed good to excellent conversions (70−95%) for the hydroamination of terminal acetylenes, namely, phenylacetylene, *t*-butylacetylene, and cyclohexylacetylene, with a series of primary and secondary amines at 5 mol % of the precatalyst loading at 40−100 °C in 7−24 h of the reaction time.[27] Another example involved the N-heterocyclic carbene ligands, namely, 1,3-*di*methyl-imidazol-2-ylidene and [1,3-*di*-(2,4,6-*tri*methylphenyl)-imidazol-2-ylidene], in conjunction with Ti(NMe$_2$)$_4$[29] carried out the alkyne hydroamination reactions under "Ligand Assisted Catalysis (LAC)" conditions at a much higher 10 mol % of the catalyst loading. In this regard it is worth pointing out that the hydroamination reaction employing the gold **1c**−**4c** precatalysts were performed at a much lower catalyst loading of 2 mol % compared to the aforementioned reports where higher loadings of 5−10 mol % were used.

Besides the N-heterocyclic carbene based precatalysts, various other transition metal based initiators like AuCl$_3$,[30] Ti(NMe$_2$)$_4$,[31] V(NMe$_2$)$_4$,[32] lanthanides and actinides,[33] and so forth have been reported for the intermolecular hydroamination of terminal alkynes displaying comparable activity to the gold(I) (**1c**−**4c**) precatalysts. Of the gold based precatalysts for the intermolecular hydroamination of terminal alkynes that exist, notable is the [Au(TPP)]Cl (TPP = tetraphenylporphyrin) complex that carried out hydroamination reaction of *p*-methoxyaniline to phenylacetylene at 5 mol % of the precatalyst loading at 80 °C in 12 h of the reaction time.[34] Another Au(III) precatalyst is AuCl$_3$, which in presence of AgOTf exhibited good activity for intermolecular hydroamination of terminal alkynes with aniline derivatives at room temperature at 5 mol % of the precatalyst loading.[30] The **1c**−**4c** complexes were, however, less active

(29) Takaki, K.; Koizumi, S.; Yamamoto, Y.; Komeyama, K. *Tetrahedron Lett*. **2006**, *47*, 7335–7337.

(30) Luo, Y.; Li, Z.; Li, C.-J. *Org. Lett*. **2005**, *7*, 2675–2678.
(31) Shi, Y.; Ciszewski, J. T.; Odom, A. L. *Organometallics* **2001**, *20*, 3967–3969.
(32) Lorber, C.; Choukroun, R.; Vendier, L. *Organometallics* **2004**, *23*, 1845–1850.
(33) Haskel, A.; Straub, T.; Eisen, M. S. *Organometallics* **1996**, *15*, 3773–3775.
(34) Zhou, C.-Y.; Chan, P. W. H.; Che, C.-M. *Org. Lett*. **2006**, *8*, 325–328.

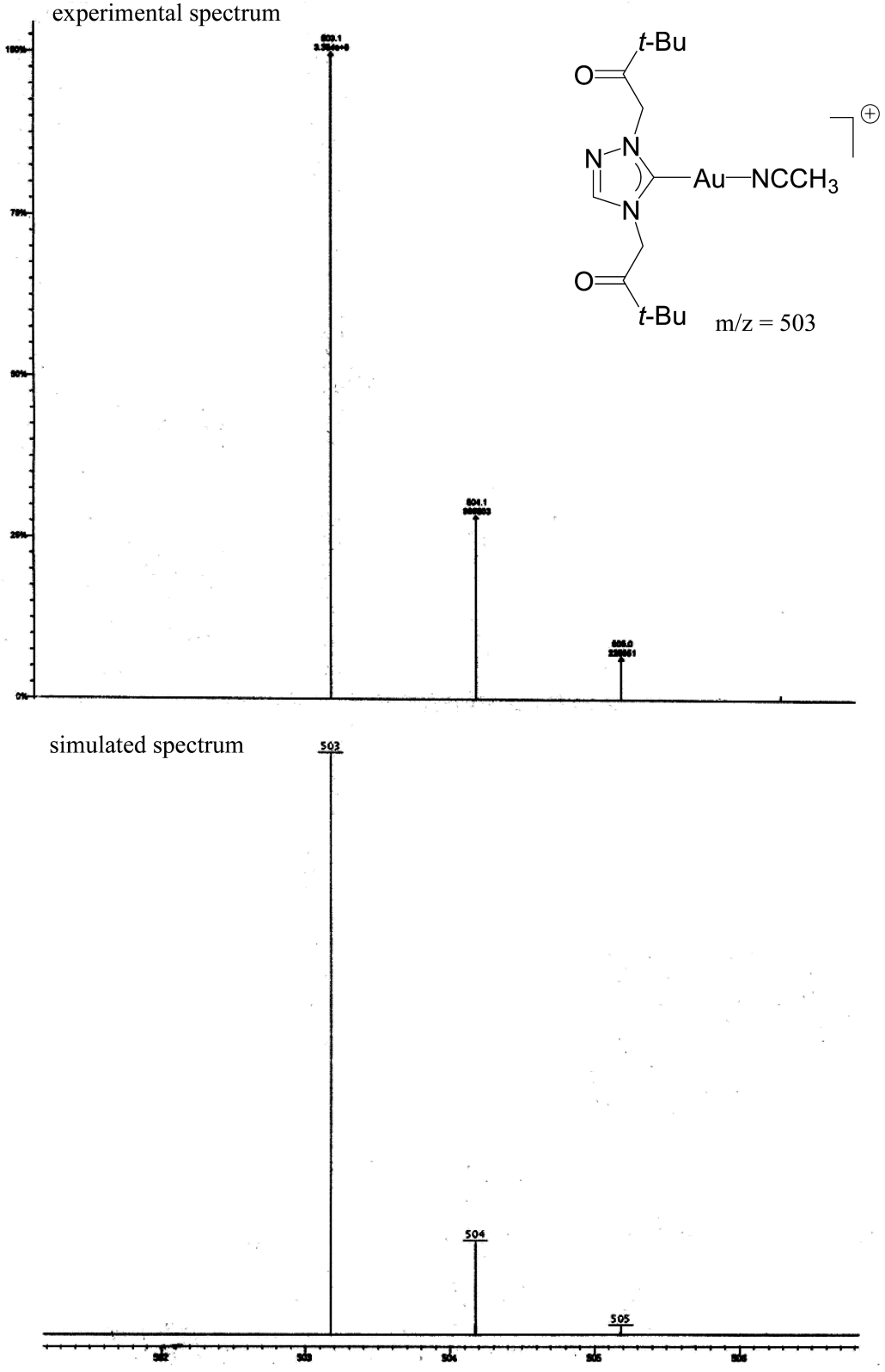

Figure 7. Overlay of experimental and simulated LCMS−ESI mass spectrum in CH_3CN showing isotopic distribution of acetonitrile coordinated species of **3c**.

than a gold(I) based precatalyst,[35] $(Ph_3P)AuCH_3$, which at 0.01−0.5 mol % catalyst loading in presence of an acidic promoter $H_3PW_{12}O_{40}$, exhibited extremely high turnover numbers (TONs) up to 9000 for hydroamination of a neat mixture of a variety of alkynes with several aniline derivatives at 70 °C in 0.25−24 h.

Of particular interest is the mechanism of the intermolecular hydroamination of terminal alkynes by a late-transition metal that generally proceeds via an alkyne activation pathway, of which mainly two views persist. One involving a

(35) Mizushima, E.; Hayashi, T.; Tanaka, M. *Org. Lett.* **2003**, *5*, 3349–3352.

direct intermolecular nucleophilic attack by the amine on the alkyne bound to the gold center; however, this route is less likely as anilines with more electron-withdrawing substituents were reported to react faster.[11c,35] Consequently, the other more probable route involves coordination of the aniline to the gold prior to the C−N bond formation. As the catalysis was performed at 90 °C, the thermal stability of the **1c**−**4c** precatalysts at this temperature was examined both in the solid state by thermogravimetric analysis (See Supporting Information, Figure S14) and in solution by ^{1}H NMR analysis (See Supporting Information, Figures S15−S18). Indeed, both the thermogravimetric analysis and ^{1}H NMR results suggested the **1c**−**4c** precatalysts to be stable at the hydroamination catalysis temperature of 90 °C.

On the basis of the above observations a proposed mechanism (Scheme 3) involve the generation of the solvent coordinated active species [(NHC)Au(CH$_3$CN)]$^+$BF$_4^-$ (**A**) from the precatalyst **1c**−**4c** by treatment with AgBF$_4$ in acetonitrile accompanied by the precipitation of AgCl. The formation of the solvent coordinated active species [(NHC)-Au(CH$_3$CN)]$^+$BF$_4^-$ (**A**), for a representative precatalyst **3c**, was corroborated by mass spectrometric studies (Figure 7 and Supporting Information, Figure S19).[36] The acetonitrile adduct species (**A**), from the representative precatalyst **3c**, was found to be stable in solution at hydroamination reaction temperature of 90 °C as observed in the LCMS−ESI experiment (See Supporting Information, Figure S20). The reaction of active species **A** with terminal alkyne (RC≡CH) would result in the formation of alkyne coordinated species [(NHC)Au(alkyne)]$^+$BF$_4^-$ (**B**) which on reaction with an aryl amine would result in [(NHC)Au(amine)(alkyne)]$^+$BF$_4^-$ intermediate (**C**). The species **C** then would undergo hydroamination of the coordinated alkyne to give alkene coordinated species [(NHC)Au(alkene)]$^+$BF$_4^-$ (**D**). Indeed, the DFT calculations performed on the hydroamination of terminal alkynes with aryl amines showed the Markovnikov product to be more stable than the anti-Markovnikov addition product (See Supporting Information, Figure S21 and Tables S20−S60). Similar Markovnikov type addition for hydroamination of terminal alkynes with arylamines has been reported earlier.[11a,27,37] Also the stereospecificity of the hydroamination reaction, established by the isolation and subsequent characterization of hydroaminated products for a representative precatalyst **1c**, showed Markovnikov type addition occurring on the activated terminal alkyne. The species **D** would finally yield the desired ketimine product through tautomerism along with the regeneration of active species **A**.

Conclusions

In summary, a series of new highly convenient gold **1c**−**4c** precatalysts supported over *N*/*O*-functionalized 1,2,4-triazole based N-heterocyclic carbenes for intermolecular hydroamination of terminal alkynes with *o*/*p*-substituted arylamines yielding ketimines in air have been successfully designed. These gold(I) precatalysts **1c**−**4c** were found to be significantly more active than their silver analogues **1b**−**4b** thereby highlighting the importance of gold as a metal in the catalysis. Comparison of the gold(I) **1c**−**4c** precatalysts with the gold complexes of imidazole based N-heterocyclic carbene analogues, namely, [1-(benzyl)-3-(*N*-*t*-butylacetamido)-imidazol-2-ylidene]AuCl and [1-(2-hydroxy-cyclohexyl)-3-(benzyl)imidazol-2-ylidene]AuCl, further established the importance of 1,2,4-triazole based N-heterocyclic carbene in stabilizing the highly active gold precatalysts **1c**−**4c** for the alkyne hydroamination reaction.

Experimental Section

General Procedures. All manipulations were carried out using standard Schlenk techniques. Solvents were purified and degassed by standard procedures. 3,3-Dimethyl-2-oxobutyl-1,2,4-triazole,[38] 2-hydroxy-cyclohexyl-1,2,4-triazole[39] and (SMe$_2$)-AuCl[40] were synthesized according to modified literatures procedures. The synthesis of 1-(*N*-*t*-butylacetamido)-4-(benzyl)-1,2,4-triazolium bromide (**2a**) was reported earlier.[16c] ^{1}H and ^{13}C{^{1}H} NMR spectra were recorded in CDCl$_3$ on a Varian 400 MHz NMR spectrometer. ^{1}H NMR peaks are labeled as singlet (s), doublet (d), triplet (t), multiplet (m), and septet (sept). Infrared spectra were recorded on a PerkinElmer Spectrum One FT-IR spectrometer. Mass spectrometry measurements were done on a Micromass Q-Tof spectrometer. GC spectra were obtained on a PerkinElmer Clarus 600 equipped with a FID. GC-MS spectra were obtained on a PerkinElmer Clarus 600 T equipped with EI source. ESI−MS experiments were performed with a Varian Proctar 500-LCMS instrument, with upper mass limit of *m*/*z* 2000, through direct infusion via a syringe pump. Standard experimental conditions in the LCMS was at the given capillary voltage 80 V, needle voltage 5000 V, syringe pressure 10 psi, temperature 320 °C, flow rate 10 μL.min^{-1}, RF loading 80%, nebulizing gas (helium) pressure 50 psi. Elemental Analysis was carried out on Thermo Quest FLASH 1112 SERIES (CHNS) Elemental Analyzer. The thermogravimetric analysis of the **1c**−**4c** precatalysts were carried out using a Perkin-Elmer Pyris thermal analyzer in the temperature range 30−600 °C at a rate of 10 °C/min under nitrogen flow (flow rate: 10 mL/min). X-ray diffraction data for compounds **1b**, **2b**, and **1c**−**4c** were collected on an Oxford Diffraction XCALIBUR-S diffractometer, and crystal data collection and refinement parameters are summarized in the Supporting Information, Table S1. The structures were solved using direct methods and standard difference map techniques, and were refined by full-matrix least-squares procedures on F^2 with SHELXTL (Version 6.10).[41]

Synthesis of 1-(3,3-Dimethyl-2-oxobutyl)-4-(benzyl)-1,2,4-triazolium Bromide (1a). A mixture of 3,3-dimethyl-2-oxobutyl-1,2,4-triazole (0.680 g, 4.07 mmol) and benzyl bromide (0.696 g, 4.07 mmol) in acetonitrile (ca. 5 mL) was refluxed for 6 h, after which the solvent was removed under vacuum. The reaction mixture was washed in hot petroleum ether (ca. 3 × 15 mL) and dried under vacuum to give the product **1a** as a brown viscous liquid (0.967 g, 70%). ^{1}H NMR (CDCl$_3$, 400 MHz, 25 °C): δ 11.1 (s, 1H, N−C(5)*H*-N), 9.18 (s, 1H, N−C(3)*H*-N), 7.57 (br, 2H, C$_6$*H*$_5$), 7.36 (br, 3H, C$_6$*H*$_5$), 5.88 (s, 2H, C*H*$_2$Ph), 5.81 (s, 2H, C*H*$_2$), 1.24 (s, 9H, C(C*H*$_3$)$_3$). ^{13}C{^{1}H} NMR (CDCl$_3$, 100 MHz, 25 °C): δ 204.8 (*C*O), 144.2 (N-*C*(5)H−N), 143.8 (N-*C*(3)H−N), 132.1 (*ipso*-*C*$_6$H$_5$), 129.8 (*o*-*C*$_6$H$_5$), 129.6 (*m*-*C*$_6$H$_5$), 129.2 (*p*-*C*$_6$H$_5$), 57.4 (*C*H$_2$Ph), 52.1 (*C*H$_2$), 43.5 (*C*(CH$_3$)$_3$), 26.1

(36) de Frémont, P.; Marion, N.; Nolan, S. P. *J. Organomet. Chem.* **2009**, *694*, 551–560.

(37) (a) Leyva, A.; Corma, A. *Adv. Synth. Catal.* **2009**, *351*, 2876–2886. (b) Corma, A.; Concepción, P.; Domínguez, I.; Fornés, V.; Sabater, M. J. *J. Catal.* **2007**, *251*, 39–47.

(38) Xu, L. Z.; Jiao, K.; Zhang, S. S.; Kuang, S. P. *Bull. Korean Chem. Soc.* **2002**, *23*, 1699–1701.

(39) Murabayashi, A.; Makisumi, Y. *Heterocycles* **1990**, *31*, 537–548.

(40) Brandys, M.-C.; Jennings, M. C.; Puddephatt, R. J. *J. Chem. Soc., Dalton Trans.* **2000**, 4601–4606.

(41) (a) Sheldrick, G. M. *SHELXL-97, Program for refinement of crystal structures*; University of Göttingen: Göttingen, Germany, 1997. (b) Sheldrick, G. M. *SHELXS-97, Structure solving program*; University of Göttingen: Göttingen, Germany, 1997.

($C(\underline{C}H_3)_3$). IR data (cm^{-1}) KBr pellet: 1732 (s) ($\nu_{C=O}$). HRMS (ES): m/z 258.1606 $[(NHC)+H]^+$, Calcd. 258.1606. Anal. Calcd. for $C_{15}H_{20}N_3OBr$: C, 53.26; H, 5.96; N, 12.42. Found: C, 53.05; H, 5.92; N, 12.17%.

Synthesis of [1-(3,3-Dimethyl-2-oxobutyl)-4-(benzyl)-1,2,4-triazol-5-ylidene]AgBr (1b). A mixture of 1-(3,3-dimethyl-2-oxobutyl)-4-(benzyl)-1,2,4-triazolium bromide (**1a**) (0.436 g, 1.29 mmol) and Ag_2O (0.150 g, 0.645 mmol) in acetonitrile (ca. 30 mL) was stirred at room temperature for 4 h. The reaction mixture was filtered, and the solvent was removed under vacuum to give the product **1b** as an off white solid (0.289 g, 50%). Single crystals for X-ray diffraction studies were grown from the mixture of chloroform and acetonitrile employing a slow evaporation technique. ^{1}H NMR ($CDCl_3$, 400 MHz, 25 °C): δ 7.88 (s, 1H, N−C(3)$\underline{H}$-N), 7.25 (br, 5H, $C_6\underline{H}_5$), 5.72 (s, 2H, $C\underline{H}_2$Ph), 5.37 (s, 2H, $C\underline{H}_2$), 1.22 (s, 9H, $C(C\underline{H}_3)_3$). $^{13}C\{^1H\}$ NMR ($CDCl_3$, 100 MHz, 25 °C): δ 207.8 ($\underline{C}O$), 187.9 (Ag−N$\underline{C}$N), 141.9 (N-$\underline{C}$(3)H−N), 135.0 (*ipso*-$\underline{C}_6H_5$), 129.1 (*o*-$\underline{C}_6H_5$), 128.5 (*m*-$\underline{C}_6H_5$), 128.3 (*p*-$\underline{C}_6H_5$), 58.1 ($\underline{C}H_2$Ph), 52.7 ($\underline{C}H_2$), 43.3 ($\underline{C}(CH_3)_3$), 26.3 ($C(\underline{C}H_3)_3$). IR data (cm^{-1}) KBr pellet: 1723 (s) ($\nu_{C=O}$). Anal. Calcd. for $C_{15}H_{19}N_3OAgBr$: C, 40.48; H, 4.30; N, 9.44. Found: C, 39.60; H, 4.17; N, 9.82%.

Synthesis of [1-(3,3-Dimethyl-2-oxobutyl)-4-(benzyl)-1,2,4-triazol-5-ylidene]AuCl (1c). A mixture of [1-(3,3-dimethyl-2-oxobutyl)-4-(benzyl)-1,2,4-triazol-5-ylidene]AgBr (**1b**) (0.173 g, 0.390 mmol) and $(SMe_2)AuCl$ (0.115 g, 0.390 mmol) in acetonitrile (ca. 30 mL) was stirred at room temperature for 4 h when the formation of an off-white AgBr precipitate was observed. The reaction mixture was filtered, and the solvent was removed under vacuum to give the product **1c** as an off white solid (0.145 g, 76%). Single crystals for X-ray diffraction studies were grown from the mixture of chloroform and acetonitrile employing a slow evaporation technique. ^{1}H NMR ($CDCl_3$, 400 MHz, 25 °C): δ 8.00 (s, 1H, N−C(3)$\underline{H}$-N), 7.39 (br, 3H, $C_6\underline{H}_5$), 7.36 (br, 2H, $C_6\underline{H}_5$), 5.41 (s, 2H, $C\underline{H}_2$Ph), 5.36 (s, 2H, $C\underline{H}_2$), 1.29 (s, 9H, $C(C\underline{H}_3)_3$). $^{13}C\{^1H\}$ NMR ($CDCl_3$, 100 MHz, 25 °C): δ 206.0 ($\underline{C}O$), 176.1 (Au−N$\underline{C}$N), 142.2 (N-$\underline{C}$(3)H−N), 133.5 (*ipso*-$\underline{C}_6H_5$), 129.6 (*o*-$\underline{C}_6H_5$), 129.5 (*m*-$\underline{C}_6H_5$), 128.4 (*p*-$\underline{C}_6H_5$), 57.0 ($\underline{C}H_2$Ph), 52.9 ($\underline{C}H_2$), 43.7 ($\underline{C}(CH_3)_3$), 26.2 ($C(\underline{C}H_3)_3$). IR data (cm^{-1}) KBr pellet: 1723 (s) ($\nu_{C=O}$). HRMS (ES): m/z 454.1180 $[(NHC)Au]^+$, Calcd. 454.1194. Anal. Calcd. for $C_{15}H_{19}N_3OAuCl$: C, 36.79; H, 3.91; N, 8.58. Found: C, 36.65; H, 3.99; N, 8.32%.

Synthesis of [1-(*N*-*t*-butylacetamido)-4-(benzyl)-1,2,4-triazol-5-ylidene]AgBr (2b). A mixture of 1-(*N*-*t*-butylacetamido)-4-(benzyl)-1,2,4-triazolium bromide (**2a**) (0.544 g, 1.54 mmol) and Ag_2O (0.178 g, 0.769 mmol) in acetonitrile (ca. 40 mL) was stirred at room temperature for 4 h. The reaction mixture was filtered, and the solvent was dried under vacuum to give the product **2b** as an off white solid (0.304 g, 43%). Single crystals for X-ray diffraction studies were grown from the mixture of chloroform and acetonitrile employing a slow evaporation technique. ^{1}H NMR ($CDCl_3$, 400 MHz, 25 °C): δ 7.91 (s, 1H, N−C(3)$\underline{H}$-N), 7.31−7.30 (m, 3H, $C_6\underline{H}_5$), 7.24 (br, 2H, $C_6\underline{H}_5$), 5.31 (s, 2H, $C\underline{H}_2$Ph), 5.21 (s, 2H, $C\underline{H}_2$), 1.33 (s, 9H, $C(C\underline{H}_3)_3$). $^{13}C\{^1H\}$ NMR ($CDCl_3$, 100 MHz, 25 °C): δ 185.9 (Ag−N$\underline{C}$N), 165.2 ($\underline{C}$ONH), 142.2 (N-$\underline{C}$(3)H−N), 134.6 (*ipso*-$\underline{C}_6H_5$), 129.2 (*o*-$\underline{C}_6H_5$), 128.8 (*m*-$\underline{C}_6H_5$), 128.2 (*p*-$\underline{C}_6H_5$), 56.7 ($\underline{C}H_2$Ph), 52.8 ($\underline{C}H_2$), 51.7 ($\underline{C}(CH_3)_3$), 28.7 ($C(\underline{C}H_3)_3$). IR data (cm^{-1}) KBr pellet: 1678 (s) (ν_{CONH}). Anal. Calcd. for $C_{15}H_{20}N_4OAgBr$: C, 39.16; H, 4.38; N, 12.18. Found: C, 38.83; H, 3.95; N, 13.07%.

Synthesis of [1-(*N*-*t*-butylacetamido)-4-(benzyl)-1,2,4-triazol-5-ylidene]AuCl (2c). A mixture of [1-(*N*-*t*-butylacetamido)-4-(benzyl)-1,2,4-triazol-5-ylidene]AgBr (**2b**) (0.157 g, 0.342 mmol) and $(SMe_2)AuCl$ (0.101 g, 0.342 mmol) in acetonitrile (ca. 30 mL) was stirred at room temperature for 4 h. The reaction mixture was filtered and the solvent was removed under vacuum to give the product **2c** as an off white solid (0.126 g, 73%). Single crystals for X-ray diffraction studies were grown from the mixture of chloroform and acetonitrile employing a slow evaporation technique. ^{1}H NMR ($CDCl_3$, 400 MHz, 25 °C): δ 7.97 (s, 1H, N−C(3)$\underline{H}$-N), 7.42−7.35 (m, 5H, $C_6\underline{H}_5$), 5.86 (br, 1H, N$\underline{H}$), 5.40 (s, 2H, $C\underline{H}_2$Ph), 4.96 (s, 2H, $C\underline{H}_2$), 1.39 (s, 9H, $C(C\underline{H}_3)_3$). $^{13}C\{^1H\}$ NMR ($CDCl_3$, 100 MHz, 25 °C): δ 175.8 (Au−N$\underline{C}$N), 163.7 ($\underline{C}$ONH), 142.4 (N-$\underline{C}$(3)H−N), 133.3 (*ipso*-$\underline{C}_6H_5$), 129.7 (*o*-$\underline{C}_6H_5$), 129.6 (*m*-$\underline{C}_6H_5$), 128.6 (*p*-$\underline{C}_6H_5$), 56.0 ($\underline{C}H_2$Ph), 53.1 ($\underline{C}H_2$), 52.6 ($\underline{C}(CH_3)_3$), 28.9 ($C(\underline{C}H_3)_3$). IR data (cm^{-1}) KBr pellet: 1681 (s) (ν_{CONH}). HRMS (ES): m/z 469.1290 $[(NHC)Au]^+$, Calcd. 469.1303. Anal. Calcd. for $C_{15}H_{20}N_4OAuCl$: C, 35.69; H, 3.99; N, 11.10. Found: C, 35.22; H, 3.91; N, 11.18%.

Synthesis of 1,4-*Bis*(3,3-dimethyl-2-oxobutyl)-1,2,4-triazolium chloride (3a). A mixture of 3,3-dimethyl-2-oxobutyl-1,2,4-triazole (1.66 g, 9.92 mmol) and α-chloropinacolone (1.34 g, 9.92 mmol) in acetonitrile (ca. 10 mL) was refluxed for 8 h. A white precipitate was formed, washed in hot hexane (ca. 2 × 20 mL) and dried under vacuum to give product **3a** as a white solid (1.33 g, 44%). ^{1}H NMR ($CDCl_3$, 400 MHz, 25 °C): δ 10.6 (s, 1H, N−C(5)$\underline{H}$-N), 9.49 (s, 1H, N−C(3)$\underline{H}$-N), 6.14 (s, 2H, $C\underline{H}_2$), 5.88 (s, 2H, $C\underline{H}_2$), 1.25 (s, 18H, $C(C\underline{H}_3)_3$). $^{13}C\{^1H\}$ NMR ($CDCl_3$, 100 MHz, 25 °C): δ 206.3 ($\underline{C}O$), 205.2 ($\underline{C}O$), 145.2 (N-$\underline{C}$(5)H−N), 145.0 (N-$\underline{C}$(3)H−N), 56.9 ($\underline{C}H_2$), 53.3 ($\underline{C}H_2$), 43.3 ($\underline{C}(CH_3)_3$), 43.2 ($\underline{C}(CH_3)_3$), 26.1 ($C(\underline{C}H_3)_3$), 25.9 ($C(\underline{C}H_3)_3$). IR data (cm^{-1}) KBr pellet: 1722 (s) ($\nu_{C=O}$). HRMS (ES): m/z 266.1873 $[(NHC)+H]^+$, Calcd. 266.1869.

Synthesis of [1, 4-*Bis*(3,3-dimethyl-2-oxobutyl)-1,2,4-triazol-5-ylidene]AgCl (3b). A mixture of 1,4-*bis*(3,3-dimethyl-2-oxobutyl)-1,2,4-triazolium chloride (**3a**) (0.619 g, 2.05 mmol) and Ag_2O (0.239 g, 1.03 mmol) in acetonitrile (ca. 30 mL) was stirred for 4 h. The reaction mixture was filtered and the solvent was dried under vacuum to give the product **3b** as an off white solid (0.461 g, 55%). ^{1}H NMR ($CDCl_3$, 400 MHz, 25 °C): δ 8.11 (s, 1H, N−C(3)$\underline{H}$-N), 5.50 (s, 2H, $C\underline{H}_2$), 5.48 (s, 2H, $C\underline{H}_2$), 1.26 (s, 9H, $C(C\underline{H}_3)_3$), 1.25 (s, 9H, $C(C\underline{H}_3)_3$). $^{13}C\{^1H\}$ NMR ($CDCl_3$, 100 MHz, 25 °C): δ 207.7 ($\underline{C}O$), 207.4 ($\underline{C}O$), 186.7 (Ag−N$\underline{C}$N), 143.7 (N-$\underline{C}$(3)H−N), 57.5 ($\underline{C}H_2$), 53.3 ($\underline{C}H_2$), 43.5 ($\underline{C}(CH_3)_3$), 43.4 ($\underline{C}(CH_3)_3$), 26.3 ($C(\underline{C}H_3)_3$), 26.2 ($C(\underline{C}H_3)_3$). IR data (cm^{-1}) KBr pellet: 1722 (s) ($\nu_{C=O}$). Anal. Calcd. for $C_{14}H_{23}N_3O_2AgCl$: C, 41.15; H, 5.67; N, 10.28. Found: C, 41.46; H, 5.73; N, 11.01%.

Synthesis of [1, 4-*Bis*(3,3-dimethyl-2-oxobutyl)-1,2,4-triazol-5-ylidene]AuCl (3c). A mixture of [1, 4-*bis*(3,3-dimethyl-2-oxobutyl)-1,2,4-triazol-5-ylidene]AgCl (**3b**) (0.187 g, 0.458 mmol) and $(SMe_2)AuCl$ (0.135 g, 0.458 mmol) in acetonitrile (ca. 30 mL), was stirred at room temperature for 4 h when the formation of an off-white AgCl precipitate was observed. The reaction mixture was filtered, and the solvent was removed under vacuum to give the product **3c** as an off white solid (0.139 g, 61%). Single crystals for X-ray diffraction studies were grown from the mixture of chloroform and acetonitrile employing slow evaporation technique. ^{1}H NMR ($CDCl_3$, 400 MHz, 25 °C): δ 8.09 (s, 1H, N−C(3)$\underline{H}$-N), 5.35 (s, 2H, $C\underline{H}_2$), 5.27 (s, 2H, $C\underline{H}_2$), 1.31 (s, 9H, $C(C\underline{H}_3)_3$), 1.29 (s, 9H, $C(C\underline{H}_3)_3$). $^{13}C\{^1H\}$ NMR ($CDCl_3$, 100 MHz, 25 °C): δ 206.0 ($\underline{C}O$), 205.7 ($\underline{C}O$), 177.2 (Au−N$\underline{C}$N), 143.7 (N-$\underline{C}$(3)H−N), 57.0 ($\underline{C}H_2$), 52.8 ($\underline{C}H_2$), 43.9 ($\underline{C}(CH_3)_3$), 43.8 ($\underline{C}(CH_3)_3$), 26.4 ($C(\underline{C}H_3)_3$), 26.3 ($C(\underline{C}H_3)_3$). IR data (cm^{-1}) KBr pellet: 1724 (s) ($\nu_{C=O}$). HRMS (ES): m/z 462.1442 $[(NHC)-Au]^+$, Calcd. 462.1456. Anal. Calcd. for $C_{14}H_{23}N_3O_2AuCl$: C, 33.78; H, 4.66; N, 8.44. Found: C, 33.44; H, 4.67; N, 8.62%.

Synthesis of 1-(2-Hydroxy-cyclohexyl)-4-(benzyl)-1,2,4-triazolium bromide (4a). A mixture of 2-hydroxy-cyclohexyl-1,2,4-triazole (6.55 g, 39.2 mmol) and benzyl bromide (6.70 g, 39.2 mmol) in dichloromethane (ca. 15 mL) was refluxed for 10 h. The mixture was cooled to room temperature, and the solvent was removed under vacuum. The mixture was washed with acetone (ca. 2 × 30 mL) and dried under vacuum to give the product **4a** as a white solid (6.80 g, 51%). ^{1}H NMR ($CDCl_3$, 400 MHz, 25 °C): δ 10.9 (s, 1H, N−C(5)$\underline{H}$-N), 8.48 (s, 1H, N−C(3)$\underline{H}$-N), 7.61−7.58 (m, 2H, $C_6\underline{H}_5$), 7.45−7.40 (m, 3H, $C_6\underline{H}_5$), 5.81 (d, 1H, $^2J_{HH}$ = 14 Hz, $C\underline{H}_2$), 5.69 (d, 1H, $^2J_{HH}$ = 14 Hz,

CH_2), 4.60−4.54 (m, 1H, C_6H_{10}), 3.86−3.79 (m, 1H, C_6H_{10}), 2.16−2.13 (m, 2H, C_6H_{10}), 2.04−1.93 (m, 1H, C_6H_{10}), 1.85−1.78 (m, 2H, C_6H_{10}), 1.56−1.33 (m, 3H, C_6H_{10}). $^{13}C\{^1H\}$ NMR ($CDCl_3$, 100 MHz, 25 °C): δ 143.2 (N-*C*(5)H−N), 142.8 (N-*C*(3)H−N), 132.0 (*ipso*-C_6H_5), 129.9 (*o*-C_6H_5), 129.8 (*m*-C_6H_5), 129.7 (*p*-C_6H_5), 71.3 (C_6H_{10}), 69.0 (C_6H_{10}), 52.4 (CH_2), 34.0 (C_6H_{10}), 29.8 (C_6H_{10}), 24.4 (C_6H_{10}), 24.1 (C_6H_{10}). IR data (cm^{-1}) KBr pellet: 3305(s), 3101(m), 3044(s), 2987(m), 2940(s), 2863(m), 1579(m), 1519(w), 1497(s), 1450(m), 1424(w), 1407(m), 1367(w), 1280(m), 1261(m), 1234(w), 1150(m), 1136(m), 1068(s), 957(m), 872(w), 785(w), 753(m), 709(s), 616(m). HRMS (ES): *m*/*z* 258.1601 $[(NHC)+H]^+$, Calcd. 258.1606. Anal. Calcd. for $C_{15}H_{20}N_3OBr$: C, 53.26; H, 5.96; N, 12.42. Found: C, 53.47; H, 5.92; N, 12.12%.

Synthesis of {[1-(2-Hydroxy-cyclohexyl)-4-(benzyl)-1,2,4-triazol-5-ylidene]$_2$Ag}$^+$Br$^-$ (4b). A mixture of 1-(2-hydroxy-cyclohexyl)-4-(benzyl)-1,2,4-triazolium bromide (**4a**) (0.919 g, 2.72 mmol) and Ag_2O (0.316 g, 1.36 mmol) in acetonitrile (ca. 30 mL) was stirred at room temperature for 4 h. The reaction mixture was filtered, and the solvent was removed under vacuum to give the product **4b** as an off white solid (0.614 g, 64%). ^1H NMR ($CDCl_3$, 400 MHz, 25 °C): δ 7.91 (s, 2H, N−C(3)*H*-N), 7.31−7.29 (m, 10H, C_6H_5), 5.48 (d, 2H, $^2J_{HH}$ = 14 Hz, CH_2), 5.26 (d, 2H, $^2J_{HH}$ = 14 Hz, CH_2), 4.84−4.77 (m, 2H, C_6H_{10}), 3.82−3.76 (m, 2H, C_6H_{10}), 2.14−2.11 (m, 2H, C_6H_{10}), 1.78−1.75 (m, 6H, C_6H_{10}), 1.63−1.54 (m, 2H, C_6H_{10}), 1.48−1.33 (m, 6H, C_6H_{10}). $^{13}C\{^1H\}$ NMR ($CDCl_3$, 100 MHz, 25 °C): δ 184.4 (Ag−NCN), 142.2 (N-*C*(3)H−N), 135.2 (*ipso*-C_6H_5), 129.2 (*o*-C_6H_5), 128.7 (*m*-C_6H_5), 128.3 (*p*-C_6H_5), 72.5 (C_6H_{10}), 68.7 (C_6H_{10}), 52.8 (CH_2), 34.5 (C_6H_{10}), 31.6 (C_6H_{10}), 24.8 (C_6H_{10}), 24.6 (C_6H_{10}). IR data (cm^{-1}) KBr pellet: 3392(s), 3109(w), 3032(w), 2935(s), 2858(s), 1650(m), 1537(m), 1496(w), 1448(s), 1348(s), 1223(m), 1163(w), 1072(s), 959(m), 871(w), 808(w), 759(w), 716(s), 655(w), 559(w), 505(w). Anal. Calcd. for $C_{30}H_{38}N_6O_2AgBr$: C, 51.30; H, 5.45; N, 11.96. Found: C, 51.26; H, 5.52; N, 12.00%.

Synthesis of [1-(2-hydroxy-cyclohexyl)-4-(benzyl)-1,2,4-triazol-5-ylidene]AuCl (4c). A mixture of {[1-(2-hydroxy-cyclohexyl)-4-(benzyl)-1,2,4-triazol-5-ylidene]$_2$Ag}$^+$Br$^-$ (**4b**) (0.204 g, 0.291 mmol) and (SMe_2)AuCl (0.172 g, 0.583 mmol) in acetonitrile (ca. 30 mL) was stirred at room temperature for 4 h when the formation of an off-white AgBr precipitate was observed. The reaction mixture was filtered, and the solvent was dried under vacuum to give the product **4c** as an off white solid (0.171 g, 60%). Single crystals for X-ray diffraction studies were grown from the acetonitrile employing a slow evaporation technique. ^1H NMR ($CDCl_3$, 400 MHz, 25 °C): δ 7.90 (s, 1H, N−C(3)*H*-N), 7.42−7.36 (br, 5H, C_6H_5), 5.47 (d, 1H, $^2J_{HH}$ = 15 Hz, CH_2), 5.36 (d, 1H, $^2J_{HH}$ = 15 Hz, CH_2), 4.62−4.55 (m, 1H, C_6H_{10}), 4.08−4.02 (m, 1H, C_6H_{10}), 2.19−2.15 (m, 1H, C_6H_{10}), 2.08−2.05 (m, 1H, C_6H_{10}), 1.85−1.83 (m, 3H, C_6H_{10}), 1.45−1.37 (m, 3H, C_6H_{10}). $^{13}C\{^1H\}$ NMR (DMSO-d_6, 100 MHz, 25 °C): δ 171.8 (Au−NCN), 143.4 (N-*C*(3)H−N), 135.2 (*ipso*-C_6H_5), 128.5 (*o*-C_6H_5), 128.0 (*m*-C_6H_5), 127.6 (*p*-C_6H_5), 70.3 (C_6H_{10}), 68.4 (C_6H_{10}), 51.3 (CH_2), 34.0 (C_6H_{10}), 31.2 (C_6H_{10}), 24.0 (C_6H_{10}), 23.5 (C_6H_{10}). IR data (cm^{-1}) KBr pellet: 3472(s), 3108(m), 3044(w), 2939(s), 2864(m), 2225(w), 1538(m), 1447(s), 1235(m), 1068(s), 1003(w), 958(m), 900(w), 808(w), 754(w), 724(m), 599(w). HRMS (ES): *m*/*z* 454.1183 $[(NHC)Au]^+$, Calcd. 454.1194. Anal. Calcd. for $C_{15}H_{19}N_3OAuCl$: C, 36.79; H, 3.91; N, 8.58. Found: C, 37.14; H, 4.08; N, 8.24%.

Computational Methods

The density functional theory calculations were performed on the following silver(I) and gold(I) (NHC)MX (M = Ag, Au, X = Br, Cl) type species, **1b**, **2b**, and **1c**−**4c** using the GAUSSIAN 03[42] suite of quantum chemical programs. The Becke three parameter exchange functional in conjunction with Lee−Yang−Parr correlation functional (B3LYP) has been employed in this study.[43,44] Stuttgart−Dresden effective core potential (ECP), representing 19 core electrons, along with valence basis set; SDD is used for silver[45] and gold[46] and all other atoms are treated with 6-31G(d) basis set.[47] All stationary points are characterized as minima by evaluating Hessian indices on the respective potential energy surfaces. Tight SCF convergence (10^{-8} a.u.) was used for all calculations. Natural bond orbital (NBO) analysis[48] was performed using the NBO 3.1 program implemented in the GAUSSIAN 03 package.

Inspection of the metal−ligand donor−acceptor interactions was carried out using CDA.[49] CDA is a valuable tool in analyzing the interactions between molecular fragments on a quantitative basis, with an emphasis on the electron donation.[50] The orbital contributions in the geometry optimized silver(I) and gold(I) (NHC)MX (M = Ag, Au, X = Br, Cl) type species, **1b**, **2b**, and **1c**−**4c** can be divided into three parts:

(i) σ—donation from the [NHC→MX], M = Ag, Au, X = Br, Cl fragment
(ii) π—back-donation from [NHC←MX], M = Ag, Au, X = Br, Cl fragment
(iii) repulsive polarization (*r*)

The CDA calculations are performed using the program AOMix,[51] and using the B3LYP/SDD, 6-31G(d) wave function for **1b**, **2b**, and **1c**−**4c**. Molecular orbital (MO) compositions and the overlap populations were calculated using the AOMix Program. The analysis of the MO compositions in terms of occupied and unoccupied fragment orbitals (OFOs and UFOs, respectively), construction of orbital interaction diagrams, the CDA was performed using the AOMix-CDA.[52]

Further DFT calculations were also performed on the Markovnikov and anti-Markovnikov products of the hydroamination of terminal alkynes with aryl amines at B3LYP/6-31G* level of theory.

General Procedure for the Hydroamination of Alkynes. In a typical run, a Schlenk flask was charged with a mixture of complexes **1b** or **2b** or **3b** or **4b** or **1c** or **2c** or **3c** or **4c** (2 mol %, 0.01 mmol), $AgBF_4$ (2 mol %, 0.01 mmol), and acetonitrile (ca. 5 mL) and to this was added the mixture of arylamines, alkynes, and diethyleneglycol-di-*n*-butyl ether (internal standard) in a molar ratio of 1:1.5:1 (See Table 1). The reaction mixture was heated at 90 °C for 12 h in air, after which it was filtered and the product was analyzed by gas chromatography using diethyleneglycol-di-*n*-butyl ether as an internal standard.

General Procedure of Control Experiments for the Hydroamination of Alkynes. In a typical run, a Schlenk flask was charged

(42) Frisch, M. J. et al. *GAUSSIAN 03*, Revision C.02; Gaussian, Inc.: Wallingford, CT, 2004.
(43) Becke, A. D. *Phys. Rev. A* **1988**, *38*, 3098–3100.
(44) Lee, C.; Yang, W.; Parr, R. G. *Phys. Rev. B* **1988**, *37*, 785–789.
(45) (a) Alkauskas, A.; Baratoff, A.; Bruder, C. *J. Phys. Chem. A* **2004**, *108*, 6863–6868. (b) Andrae, D.; Häussermann, U.; Dolg, M.; Stoll, H.; Preuss, H. *Theor. Chim. Acta* **1990**, *77*, 123–141.
(46) (a) Wang, X.; Andrews, L. *J. Am. Chem. Soc.* **2001**, *123*, 12899–12900. (b) Faza, O. N.; López, C. S.; Álvarez, R.; de Lera, A. R. *J. Am. Chem. Soc.* **2006**, *128*, 2434–2437.
(47) Hehre, W. J.; Ditchfield, R.; Pople, J. A. *J. Chem. Phys.* **1972**, *56*, 2257–2261.
(48) Reed, A. E.; Curtiss, L. A.; Weinhold, F. *Chem. Rev.* **1988**, *88*, 899–926.
(49) Dapprich, S.; Frenking, G. *J. Phys. Chem.* **1995**, *99*, 9352–9362.
(50) (a) Vyboishchikov, S. F.; Frenking, G. *Chem.—Eur. J.* **1998**, *4*, 1439–1448. (b) Frenking, G.; Pidun, U. *J. Chem. Soc., Dalton Trans.* **1997**, 1653–1662.
(51) Gorelsky, S. I. *AOMix: Program for Molecular Orbital Analysis*; York University: Toronto, Canada, 1997; http://www.sg-chem.net/ (accessed June 27, 2009).
(52) Gorelsky, S. I.; Ghosh, S.; Solomon, E. I. *J. Am. Chem. Soc.* **2006**, *128*, 278–290.

Table 1. Selected Results of Hydroamination of Alkynes Catalyzed by **1b**−**4b**, **1c**−**4c**, and Gold Complexes of Imidazole Based N-heterocyclic Carbenes[a]

				Silver(I)				gold(I)					
entry	reagent	reagent	product	**1b** Yield[b]	**2b** Yield[b]	**3b** Yield[b]	**4b** Yield[b]	**1c** Yield[b]	**2c** Yield[b]	**3c** Yield[b]	**4c** Yield[b]	*c* Yield[b]	*d* Yield[b]
1			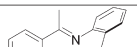	9	1	4	2	42	46	66	52	11	22
2			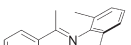	2	5	5	0	88	81	91	62	20	23
3		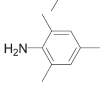	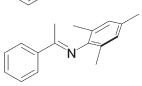	7	0	16	1	84	75	80	58	16	46
4			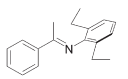	4	2	1	2	81	77	92	73	24	33
5			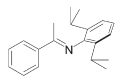	8	3	6	1	81	69	84	70	21	21
6	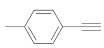	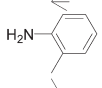	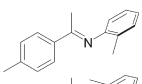	1	16	4	3	56	46	46	52	32	17
7	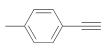		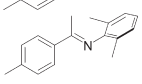	4	10	1	5	93	69	88	75	40	30
8	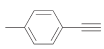		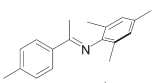	6	7	29	20	93	69	87	71	47	46
9	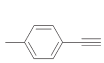		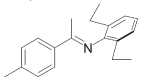	8	3	3	1	83	78	78	87	34	37
10	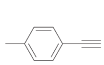		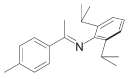	5	6	1	1	81	69	78	66	33	26
11			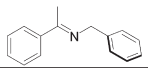	1	1	1	1	1	1	2	1	1	1

[a] See refs in footnotes c and d. Reaction conditions: 0.50 mmol of aryl/alkyl amine, 0.75 mmol of alkyne, 2 mol % of catalyst **1b**−**4b** or **1c**−**4c** or gold complexes of imidazole based N-heterocyclic carbenes, 2 mol % $AgBF_4$ and 5 mL of CH_3CN at 90 °C (12 h) in air. [b] The yields (%) were determined by GC using diethylene glycol di-*n*-butyl ether as an internal standard. [c] Ray, L.; Shaikh, M. M.; Ghosh, P. *Inorg. Chem.* **2008**, *47*, 230−240. [d] Ray, L.; Katiyar, V.; Barman, S.; Raihan, M. J.; Nanavati, H.; Shaikh, M. M.; Ghosh, P. *J. Organomet. Chem.* **2007**, *692*, 4259−4269. .

Scheme 3

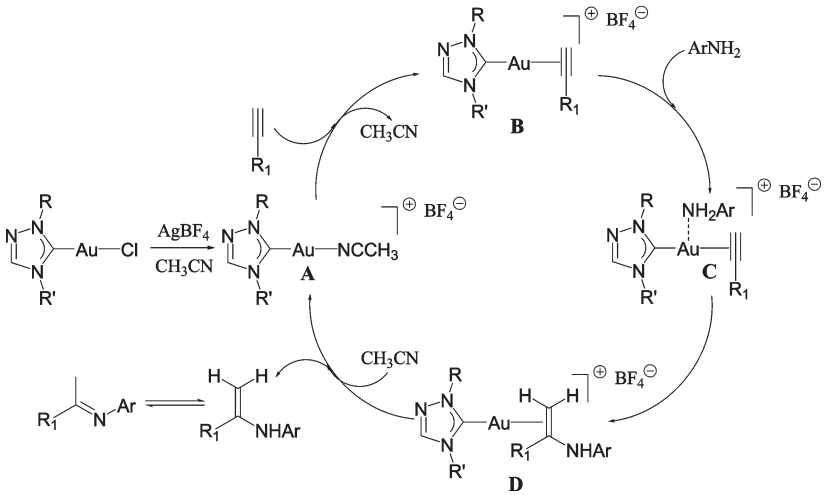

with a mixture of $(SMe_2)AuCl/AgBF_4$ (2 mol %) or [1-(benzyl)-3-*N*-*t*-butylacetamido)imidazol-2-ylidene]AuCl[12c]/$AgBF_4$ (2 mol %) or [1-(2-hydroxy-cyclohexyl)-3-(benzyl)-imidazol-2-ylidene]AuCl[10f]/$AgBF_4$ (2 mol %) and acetonitrile (ca. 5 mL) and to this was added the mixture of arylamines, alkynes, and diethyleneglycol-di-*n*-butyl ether (internal standard) in a molar ratio of 1:1.5:1 (See Table 1 and Supporting Information, Table S18). The reaction mixture was heated at 90 °C for 12 h in air, after which it was filtered and the product was analyzed by gas chromatography using diethyleneglycol-di-*n*-butyl ether as an internal standard.

General Procedure of Blank Experiments. In a typical run, a Schlenk flask was charged with the mixture of arylamines, alkynes, and diethyleneglycol-di-*n*-butyl ether (internal standard) in a molar ratio of 1:1.5:1 and $AgBF_4$ (2 mol %) and acetonitrile (ca. 5 mL) (See Supporting Information, Table S18). The reaction mixture was heated at 90 °C for 12 h in air, after which it was filtered and the product was analyzed by gas chromatography using diethyleneglycol-di-*n*-butyl ether as an internal standard.

Mercury-Poisoning Experiment. A Schlenk flask was charged with a mixture of a representative complex **1c** (2 mol %, 0.01 mmol), $AgBF_4$ (2 mol %, 0.01 mmol), excess Hg(0) ($\sim$ 100 times with respect to the catalyst loading), and acetonitrile (ca. 5 mL) and to this was added the mixture of aryl amines, alkynes, and diethyleneglycol-di-*n*-butyl ether (internal standard) in a molar ratio of 1:1.5:1 (See Supporting Information, Table S18). The reaction mixture was heated at 90 °C for 12 h in air, after which it was filtered and the product was analyzed by gas chromatography using diethyleneglycol-di-*n*-butyl ether as an internal standard.

^{1}H NMR Experiment on the Stability the 1c−4c Complexes at 90 °C. A solution of **1c**−**4c** in DMSO-d6 (0.6 mL) in an NMR tube was heated at 90 °C and was monitored by ^{1}H NMR spectroscopy at different intervals of time (0, 1, and 12 h). No significant change in the ^{1}H NMR resonances was observed as a function of time thereby attesting to the stable nature of these **1c**−**4c** complexes at 90 °C (See Supporting Information, Figures S15−S18).

ESI-MS Experiment for Detection of the Acetonitrile Coordinated Species. The electrospray ionization mass spectrometry (ESI-MS) experiment was performed in a positive ion mode to detect the proposed acetonitrile coordinated gold species of a representative precatalyst **3c** formed upon treatment with $AgBF_4$ during catalysis of the alkyne hydroamination reaction. In a typical experiment, a mixture of the precatalyst **3c** (1 equiv) and $AgBF_4$ (1 equiv) in acetonitrile was injected in the LCMS-ESI instrument, and spectrum was collected in positive ion mode. Specifically, the positive ion mode spectrum showed a peak at *m*/*z* 503 corresponding to the desired acetonitrile coordinated gold species (see Figure 7 and Supporting Information, Figure S19).

ESI-MS Experiment on the Stability of the Representative Acetonitrile Adduct Species, [{1, 4-*bis*(3,3-dimethyl-2-oxobutyl)-1,2,4-triazol-5-ylidene}Au(CH_3CN)]$^+BF_4^-$ (A). An acetonitrile adduct species, [{1, 4-*bis*(3,3-dimethyl-2-oxobutyl)-1,2,4-triazol-5-ylidene}Au(CH_3CN)]$^+BF_4^-$ (**A**), proposed to be the initiating species of the hydroamination catalytic cycle (Scheme 3), was generated by the reaction of a representative precatalyst **3c** with $AgBF_4$ in CH_3CN. The stability of the acetonitrile adduct species **A** was examined by heating the reaction mixture at 90 °C for 12 h, after which it was filtered and injected in a LCMS-ESI instrument. The ESI−MS spectrum was recorded in a positive ion mode. A peak at *m*/*z* 503 corresponded to the desired acetonitrile adduct species, [{1, 4-*bis*(3,3-dimethyl-2-oxobutyl)-1,2,4-triazol-5-ylidene}Au(CH_3CN)]$^+BF_4^-$ (**A**), and was exactly analogous to the one observed by the treatment of **3c** with $AgBF_4$ at room temperature (Supporting Information, Figure S20).

Acknowledgment. We thank Department of Science and Technology (DST), New Delhi, for financial support of this research. We are grateful to the National Single Crystal X-ray Diffraction Facility and Sophisticated Analytical Instrument Facility at IIT Bombay, India, for the crystallographic and other characterization data. Computational facilities from the IIT Bombay Computer Center are gratefully acknowledged. C.K.D. thanks CSIR-UGC, New Delhi, for a research fellowship.

Supporting Information Available: Complete reference 42, the catalysis data of **c**ontrol, blank and mercury-poisoning experiment, TGA plot, X-ray metrical data comparison table, ^{1}H and $^{13}C\{^1H\}$ NMR of silver(I) **1b**−**4b** and gold(I) **1c**−**4c** complexes. Ortep plots of **3c** and **4c**, the B3LYP coordinates of the optimized geometries for **1b**, **2b**, **1c**−**4c**, NBO tables, CDA table along with orbital interaction diagrams of **1b**, **2b**, **1c**−**4c** and the B3LYP coordinates of the Markovnikov and anti-Markovnikov products of the hydroamination reaction of terminal alkynes and aryl amines. This material is available free of charge via the Internet at http://pubs.acs.org.